Lifetime accumulation of microplastic in children and adults

Nur Hazimah Mohamed Nor*, Merel Kooi, Noël J. Diepens, Albert A. Koelmans

*Corresponding author: hazimah.mohamednor@wur.nl

This PDF file includes:

Other Supplementary Material for this manuscript includes the following:
(available at https://github.com/nhazimah/heasi)

Materials and Methods

In this section, we provide further information on the "Plastic Model" (SM1) and the "Chemical Model" (SM2). Section SM1 comprises seven subsections: auxiliary model equations (SM1-1), data collection on MP concentrations in media relevant to human intake (SM1-2), data collection for physiological characteristics (SM1-3), realignment of size ranges of plastic concentrations (SM1-4), translation of MP concentration from gut to muscle concentrations (SM1-5), goodness of fit tests for selection of PDFs (SM1-6), conversion of MP particle number to mass concentrations (SM1-7). Section SM2 comprises three subsections: physiologically based pharmacokinetic (PBPK) modelling with MERLIN Expo 3.0 (SM2-1), detailed description of the chemical leaching model (SM2-2) and chemical concentrations in plastic (SM2-3)

SM1   Plastic Model

SM1-1 Auxiliary model equations

The steady state solution to Eq. (1) from the main text, results in the steady state MP amount per capita:

$$C_{MP,SS} = \frac{(1-f_{abs}\cdot f_{a,n})\sum_{i=1}^{8}(Ir_i\cdot C_i)+(1-f_{abs})\cdot(f_{dep}\cdot InR\cdot C_a)+k_{tis}\cdot C_{tis}}{k_{loss}} \qquad (S1)$$

The MP amount egested per gram of stool per capita can be calculated based on the gut steady state concentrations:

$$C_{stool} = \frac{k_{loss}\cdot C_{MP,SS}}{M_{stool}} \qquad (S2)$$

SM1-2 Data collection on MP concentrations in media relevant to human intake

For all studies, information such as the type of analytical method used, size range of the particles identified, the percentage of positive occurrence, particle size distribution, particle shape and polymer type was collected.

If a food category is to be included in the assessment, there should at least be more than three datasets available. Each study should at least have substantial evidence that the particles are indeed MP. Secondly, consumption pattern data for the food type should be available and its relative contribution to the overall human diet of the general world population should be substantial enough (i.e., consumed in some regions). Some studies, however, do not meet these criteria for data quality and availability. For example, there is a lack of evidence for MP presence in honey as Mühlschlegel et al.[1] managed to positively identify only one particle as

PET despite their initial findings of 8 to 108 #/kg of honey through visual identification. Other food types such as seaweed nori[2], dried fish[3], and chicken gizzards[4] have been investigated for MP presence. However, these food types are not major components of the global human diet and their consumption pattern data are also not widely available. Additionally, in the case of chicken gizzards, the data quality is poor due to lack of spectroscopic identification.[5] Furthermore, based on a simple estimation, the contribution of the MPs from these food types is insignificant even on the local level. For example, the highest possible daily intake of MP from seaweed nori, which had the highest MP concentration among the food types above (max: 3000 #/kg DW), is estimated at 30 #/capita/day if it is calculated according to the average annual consumption per capita in Japan (4 kg/capita/yr).[6] This only represents ~3% and ~0.018% of the 50th and 95th percentiles of the total MP intake from other known media (Figure 3).

Criteria for each media. Seafood species were selected based on the "use and trade" information reported in the IUCN (https://www.iucnredlist.org) or "human uses" information from Fishbase. The species has to be at least used for local or national human consumption, or is commercially produced to ensure its relevance for the world population. To ensure that the reported MP concentrations in the studies are at least statistically representative of the sampled species, we set a minimum number of individuals per study sample (n=5). This criterium applied to fish, mollusc and crustaceans. One could argue that n=5 may not be representative of the species especially if there was zero occurrence of plastic in the samples. However, since we considered each food type as one category, the uncertainties from a single dataset (one species) have already been accounted for by the uncertainty of the entire dataset for that category.

As for drinking water, the data quality of the studies has recently been assessed in a review by Koelmans et al.[7]. Most of the studies associated to drinking water were evaluated to be above average with respect to the quality of sampling methodology and data reporting. Therefore, the reviewed drinking water studies (i.e., tap and bottled water) were included in our literature review. In addition, three more recent studies[8–10] were included after evaluating their sampling methodology and data reporting with the same criteria table from Koelmans et al.[7]. The datasets from Kutralam-Muniasamy et al.[11] for MP occurrence in eight brands of milk were also evaluated against the same set of criteria as drinking water. Two studies had investigated 'potential' plastic particles in beer from North America and Europe.[12,13] Both did not implement any spectroscopic methods to confirm the identity of the particles found and may even include particles of glass material. However, since beer is widely consumed, we considered the reported

concentrations from these studies noting that this is a conservative estimate for MP concentrations in beer and the outcome is not very sensitive to this assumption.

There was a limited number of studies for MP occurrence in salt and air. Therefore, we did not set any criteria for the number of replicates per sample size so that we could include as many datasets as possible. Increasing the number of datasets would improve the distribution of the MP concentrations in these media and otherwise, the uncertainty would have been accounted for in the probabilistic assessment. The selection of studies for MP intake from air was targeted on suspended atmospheric MP. Fallout or deposition studies were not considered as the size for these particulates is generally in the larger end of the range and they have a lower likelihood to be inhaled.[14]

Conversion of MP concentration per individual to per body wet weight. Plastic concentrations in fish and crustaceans were often reported on an individual basis. To allow for comparison of data from different species, the reported individual concentrations were converted to particle number per body wet weight (particles/g BWW). The weight of the sample is used for conversion if available. For studies where the weight of the samples was not reported and the length of the organisms was reported instead, the BWW was estimated from the linear correlations between log-transformed length and weight published in Fishbase[15] for that particular species. If both weight and length of the samples were not reported, the average length at first maturity (L_m) obtained from Fishbase was used to estimate the BWW. This assumption is justifiable as most studies sampled adult fish and would otherwise mention that they sampled juvenile fish. In the case of juveniles, a median size of juveniles of the species from literature is used. Detailed calculations for these MP concentration conversions are available upon request.

Determination of size ranges for each study. Microplastics have been widely defined as polymer particles of less than 5 mm. However, many studies also considered mesoplastics which are larger than 5 mm. While the upper size limits have been inconsistent for all the literature reviewed, the lower size limits of the studies have also depended largely on the analytical techniques used. To allow for comparison between studies, the size ranges for each study needs to be defined. Most studies clearly defined the size ranges of the particles which they aimed to identify or reported the size detection limits of their methodology or size range of particles which they actually found. One of these categories of information, when available, was used to set the size range for the study. However, some studies did not report any of the above in which case we assumed that the size range complied with the generally accepted definition of

"microplastics" as particles less than 5 mm[16–18] and the minimum size limit is dependent on the methodology (i.e., sieves/filter used during sample processing, microscope magnification, and sorting). For studies that carried out visual sorting under a stereomicroscope, we used their reported maximum magnification to compare against other studies with similar magnification and reported a minimum size limit. If the magnification was also not reported, we based the minimum limit as the scale bars length on the microscope images. If the study did not have any of the above, the minimum limit was set as 300 µm which was recommended by Mintenig et al.[19] as the minimum size feasible for manual sorting with forceps and 100 µm if manual sorting was not carried out but the sample was only observed and counted under a stereomicroscope, based on Lenz et al.[20].

SM1-3 Data collection for physiological characteristics

Food consumption data. To perform our MP human dietary exposure assessment, we used the food consumption data from FOSCOLLAB which is based on household surveys collated by the Food and Agriculture Organization (FAO) and World Health Organization (WHO). Some of the surveys from this database only represented a small number of consumers. Therefore, a criterium for sample size (n>5) was set for the dataset to be deemed as acceptable.

Separate statistics were available for different age groups for: all, infants and toddlers, children and adolescents, adults and elderly. As the evaluation of the MP exposure assessment in this study is over a lifetime, we classified the data into two age groups: children (1-18 years) and adult (19-70 years).

Inhalation data. The probability density functions (PDFs) defined for each age class as reported in Allan and Richardson[21] were used. The data from the categories: toddlers, children and teenagers were combined for the 'child' group, whereas the adult and senior categories were combined for the 'adult' group. The infant category was not considered in the child category as the food database in this study does not apply to infants. Subsequently, we defined the possible minimum and maximum inhalation rates of each age group and these values were either based on Stifelman[22] or on the 2.5 and 97.5 percentiles of the distributions defined by Allan and Richardson[21] (Table S3). The resulting distributions were then fitted either with normal or lognormal distributions as these are commonly used for air inhalation rates in probabilistic human health risk assessments.[23]

SM1-4 Realignment of size ranges of plastic concentrations

From our literature review, we collected 29 datasets with particle size distributions (PSDs) from 18 studies that met our minimum criterium of ≥ 5 size class bins for meaningful data fitting. When the PSDs were presented in histograms or bar graph formats, the data was extracted with WebPlotDigitizer (https://automeris.io/WebPlotDigitizer/). Size ranges >5 mm were also considered here to account for concentrations that included larger sized particles.

According to the law of fragmentation, we would expect a decreasing trend in particle abundance with increase in particle size. However, not all of the datasets assumed this trend. We speculate that this may be either due to poor recovery of smaller particles or analytical bias during visual inspection. Therefore, to avoid underestimation of particle abundances in the lower size range, we followed a similar approach as Kooi and Koelmans[24] for determining the size limits of the particle size distributions:

1. All observations with 0 abundance were excluded since it may be just an artefact of a small sample size.
2. The minimum size limit corresponded to the maximum relative abundance, following the same justification as Kooi and Koelmans[24].
3. The maximum size limit for which the dataset is valid is determined by the size before which 0 abundances is observed.

The relative abundances for each size bin were then recalculated according to the newly defined size limits for that study based on the above criteria. For datasets which had more than 5 size class bins, the following power-law function was fitted to the PSDs (Figure S1):

$$y = Cx^{-\alpha} \qquad \text{for } x \in [x_0, x_1] \qquad\qquad (S3)$$

where x is the particle size (μm), y is the relative abundance for each size, α is the power-law exponent and C is defined as a parameter depending on the limits of the distribution (min: x_0; max: x_1) and the power-law exponent:

$$C = \frac{1-\alpha}{x_1^{1-\alpha} - x_0^{1-\alpha}} \qquad \text{for } x \in [x_0, x_1]. \qquad\qquad (S4)$$

Studies which demonstrated negative regressions for log y vs log x, weak regressions based on the adjusted R^2 (<0.6) and alpha values which were less than 1, were omitted. Secondary MPs are speculated to form as a result of fragmentation of larger particles. To conform to this theory, alpha values should be greater than 1 to explain that after fragmentation of a particle, it forms

more than 1 particle.[25] The fitted parameters and regression statistics of 15 datasets from 12 studies are shown in Table S4.

SM1-5 Translation of MP concentration from gut to muscle concentrations in fish

It has been demonstrated that small MPs may likely be absorbed from the gut.[26] This absorption process may occur through several processes and may be unique for different species. To date, MP concentrations in the muscle and gut compartments of fish per unit body wet weight are available for seven fish species (Table S5).[27,28]

The muscle to gut concentration ratio ranges from 0.27 to 3.53. While Abbasi et al.[27] had ratios greater than 1 for 3 out of 4 species (i.e. indicating that there is higher MP concentrations in the muscle tissue than gut), the calculated ratios from Barboza et al.[28] were less than 1. This suggests that for some species, MPs are not easily absorbed and do not accumulate in the muscle tissue. Therefore, to account for these variations and physiological differences of other fish species, we captured the variability by implementing a normal distribution for the muscle (m) to gut (g) ratio (CF_{mg}) with mean of 1.28 ± 1.13 and the assumed MP concentrations in the muscle tissue are calculated as:

$$C_{PL} \left(\frac{\#MP}{gBWW} \text{ in muscle tissue} \right) = CF_{mg} \cdot C_{PL} \left(\frac{\#MP}{gBWW} \text{ in stomach/gut} \right) \tag{S5}$$

SM1-6 Goodness-of-fit analysis

To select the best probability density function (PDF) for the MP exposure from food and air, and the ingestion rates, the Kolmogorov-Smirnov test (KS-test) and Akaike's Information Criterion (AIC) were used simultaneously. The KS-test is generally used to check if a sample comes from a population with a specified distribution (null hypothesis). The null hypothesis is rejected if the *p*-value is less than the significance level ($p<0.05$).

The AIC is another statistical test which provides an index to compare between different fitted models. It considers the log-likelihood of the model fit (based on the standard maximum likelihood method) and the number of model parameters, penalizing when the model is overparameterized. The AIC score is calculated according to the formula:

$$AIC = -2 \cdot \log likelihood + k \cdot n_{par} \tag{S6}$$

where n_{par} represents the number of parameters in the fitted model and *k*=2 (scale parameter of the model) for the usual AIC.

The KS-test was performed for the distribution functions when fitted to the observed values and the *D* values and *p*-values are summarized in the data depository: Data S2. Several density

functions were fitted to each dataset and the AIC values are compared between models to derive the optimal density function that fits the observations.

Selection of the best distribution function to describe the observations was based on a standard procedure. Firstly, models which showed insignificant p-values ($p>0.05$), were selected as this imply that the observations are similar to the specified distribution. The D test statistic was then used to narrow down the selection of the best function to describe the distribution. This was also done simultaneously with the evaluation of the AIC values to avoid complex distribution functions.

For the selection of the distribution function to describe MP concentrations in the media, the p-values could not be considered as the data was produced after an MC simulation which adjusted for the size realignment and was hence very large (n>50 000). It is well-discussed in literature that very large samples would produce statistically significant lack of fit as the KS-test is sensitive to detecting small deviations.[29,30] However, this does not imply that the specified distribution and the observations do not come from the same distribution. Therefore, to evaluate which model describes the dataset, the model with the lowest value of the D test statistic followed by the lowest AIC value, was selected. During the selection process, simple models were preferred over complex ones such as the bimodal distributions. Test statistics for MP concentration in air were omitted here as there were too little data to verify goodness of fit of the specified distribution.

SM1-7 Conversion of MP particle numbers to mass concentrations

To convert the calculated particle numbers of MP to mass, we first collected data on extrinsic properties of the particles such as size, shape and density. The approach for PSD was discussed in the earlier section SM1-4, where we defined two power-law exponents α_{food} and α_{air}. As for shape, we identified 49 studies containing 104 datasets for food and 3 studies for air that reported particle shape distributions. The collated dataset can be found in the data depository (Data S3). Five shape categories are defined for this study: (1) fragment, (2) filament/fibre, (3) spherules/pellets, (4) film/sheet, and (5) foam. When a study reports other shape categories or paint chips, we omitted them and recalculated the proportions. The overall average proportions of each shape category ($f_{shape,all}$) for all datasets were then determined by adding all the fractions from each dataset, i ($f_{shape,i}$) and dividing by the number of datasets for that category (n).

$$f_{shape,all} = \frac{\sum_{i=1}^{n} f_{shape,i}}{n} \tag{S7}$$

Distributions of the width:length (W:L) and height:length (H:L) were then determined following the method by Kooi and Koelmans[24], where the lower and upper limits for width and height of each shape category were defined and triangular distributions were assumed. A Monte Carlo (MC) simulation of 1 000 000 iterations was performed to determine the overall respective distributions for food and air, and bimodal distribution functions were fitted using the 'mixtools' package[31] in R (Figure S2).

To obtain the polymer density distribution of the MPs found in the food and air, we collated 30 studies (i.e., 27 studies for food and 3 studies for air) which reported polymer types through spectroscopic identification (Data S4). We omitted polymer types that were not reported by more than two studies and natural polymers such as rayon and cellulose. In total, there were 15 polymer types for food and 5 polymer types for air. The lower and upper limits of the densities for these polymer types[32–35] were defined with some assumptions:

- For polyacrylate we included: poly(2-cyanoenthyl acrylate), poly(acrylic acid), poly(butyl acrylate), poly(methyl acrylate). The -methacrylates were not included[33].
- We applied the density range of polyamide (PA) to Nylon 6.
- Polystyrene acrylonitrile methyl methacrylate (Poly(styrene-co-methyl methacrylate) was assumed to have the same density as styrene methyl methacrylate, with a density ranging from 1.050 to 1.130.[35]
- For PE:PP co-polymer, only 1 density was found[34], but since this polymer accounted for less than 0.1% of the total, this was deemed as acceptable.
- Density of PU obtained from *Prospector*.[36]

Similarly, the overall proportions of each polymer type were calculated for each media. Triangular distributions were assumed for each polymer type and MC simulation of 1 000 000 iterations was performed to determine the overall density distributions for food and air respectively, and fitted with 4-modal distributions with the 'mixtools' package in R.[31] The parameters of the fitted distribution functions for the shape characteristics and densities of MP in food and air are shown in Table S7.

The PDFs of the above MP characteristics were then simulated 10 000 times. The volume per MP particle was calculated assuming an ellipsoid shape (i.e. best 'one shape fits all' approximation for MP particles)[17]:

$$V_{el} = \frac{\pi}{6} \cdot (L) \cdot (W) \cdot (H) \tag{S8}$$

where L was estimated from the PSD and W and H is estimated from the W:L and H:L ratio distributions respectively. The mass per MP particle was then calculated by multiplying the volume with the density values generated from the MC simulation. The distributions of the log-transformed mass per particle for food and air were fitted with mixture models using the 'mixtools' package in R (Figure S2 and Table S7) and evaluated with Kolmogorov-Smirnov tests (p=0.82 for food and p=0.83 for air).

The MP mass distributions in the gut were then calculated after the numerical solution of Eq. (1) with a two-step approach. Since the mass per particle distributions differ for food and air, we needed to distinguish how many particles came from each media. First, we simulated the MP number concentrations from dietary intake only. The MP number concentrations (food) were then converted to mass concentrations by multiplying with the mass per particle (food). The same procedure was performed for intake through air only. The mass concentrations are then added up to provide the total MP mass. The MP mass distributions in the gut for child and adult for each scenario of biliary excretion rates are shown in Table S10.

SM2 Chemical Model

SM2-1 PBPK model with MERLIN Expo 3.0

Chemical intake data. There are no chemical intake data for 3,3',4,4',5-pentachlorobiphenyl (PCB126), lead, di(2-ethylhexyl)phthalate (DEHP) and benzo(a)pyrene (BaP) on a world population level. Therefore, we had to use data for specific regions or countries, assuming relevance on a global level. We acquired intake data from Llobet et al.[37] for PCB126 which represents the intake from foods in Catalonia Spain. The study reported that PCB126 contributed 50.56% to total toxic equivalent (TEQ) intake. We calculated the actual daily intake of PCB126 by multiplying the estimated WHO-TEQ intake per day with the fraction contributed by PCB126 and then divided by the WHO toxicity equivalent factor (TEF) for PCB126 (TEF=0.1). We did not distinguish between genders in the present study. Therefore, we also averaged over the genders for each age group.

Lead intake data of the Italian population was used in our PBPK simulation[38]. Since the data was reported as per kilogram body weight, we used polynomial least squares regression as described by Buonanno et al.[39] to estimate the average body weight of the Italian population and subsequently calculated the daily intake per person (averaged over the genders).

For DEHP, we used the dietary intake in the German population[40] and inhalation exposure was estimated from indoor[41] and outdoor[42] air concentrations by assuming time spent

indoors:outdoors is 50:50. The body weights for children and adult of the German population[43,44] were obtained to convert the chemical intake per unit body weight to per capita.

Finally, the dietary and inhalation exposure of BaP[45,46] were based on data for the Korean population. As for the average body weight, no literature was available for the Korean population. Therefore, we had to estimate using the polynomial regression of body weight vs age which was reported for Chinese individuals[47].

PBPK parameters. The PBPK parameters used for lead and PCB126 were already pre-set in MERLIN Expo.[48] We used the PBPK parameters as reported by Chiang et al.[49] for BaP and Gentry et al.[50] for DEHP. Except for DEHP, we simulated the ingestion of chemicals as a direct input in the liver. This is because the absorption rate constants of DEHP in the stomach lumen and gut lumen were defined.

SM2-2 Description of chemical leaching model

Calculation of parameters for biphasic transfer kinetic model. Ad- and desorption to microplastic can be adequately described using a two compartment model with separate compartments and kinetic parameters for slow and fast desorption[51] (Eq. 7 and 8 in the main text). Based on Mohamed Nor and Koelmans[51], the fast-desorption compartment of a thin film of MP with a thickness (t) of 30 µm comprised 32% of the total sorption reservoir (sum of slow and fast sorption compartments) across 14 PCBs (log K_{OW} ranging from 5.24 to 7.42). For such a film, the minimum diffusion path length of the fast-sorbing fraction (d_f) can be estimated as:

$$d_f = 0.32 \times 30 = 9.6 \, \mu m \tag{S9}$$

Consequently, if the minimum dimension of the particle (d_{min}) is <9.6 µm, only fast sorption kinetics occur for that particle. However, if the minimum dimension exceeds 9.6 µm, the effective radius of the fast fraction (r_f) was set at a constant value of 4.8 µm and the slow-sorbing fraction is calculated as:

$$r_s = \frac{d_{min}}{2} - 4.8 \tag{S10}$$

The slow sorption kinetic rate constant, k_3 for the particle was then rescaled based on this effective radius of the slow-sorbing compartment (r_s) according to Fick's law of diffusion, using the average k_3 values from Mohamed Nor and Koelmans[51]:

$$k_3 = \frac{k_{3,lit} \times r_{s,lit}^2}{r_s^2} \tag{S11}$$

where $k_{3,lit}$ is 0.002 day^{-1} and $r_{s,lit}$ is 10.2 μm ($t/2 - r_f$).

The fast sorption kinetic rate constant, k_1 was based on the relationship with log K_{OW}[51]:

$$logk_1 = 0.86 \times logK_{OW} - 4.08 \tag{S12}$$

The desorption kinetic rate constant, k_2 was then estimated from the steady state solution[51]:

$$k_2 = \frac{k_1}{K_P f_1 [P]} \tag{S13}$$

where K_P was estimated based on the relationship[51]:

$$\log K_P = 0.51 \times \log K_{OW} + 1.45 \tag{S14}$$

and f_1 can be estimated as:

$$f_1 = \begin{cases} r_f / (\frac{d_{min}}{2}), & d_{min} > 9.6 \; \mu m \\ 1, & d_{min} \leq 9.6 \; \mu m \end{cases} \tag{S15}$$

SM2-3 Chemical concentrations in plastic

Based on thermodynamic principles, chemical concentrations of the plastic ingested by seafood were assumed to be equivalent to the concentrations in their lipids. To some extent, this approach represents a worst case scenario because in reality, plastic has a somewhat lower fugacity than biota lipids[52,53]. Chemical concentration data in lipids of fish and molluscs/crustaceans were thus used as proxy concentrations in plastic. We categorised the seafood into two categories; organisms found in the pelagic zone (fish) and organisms found in the littoral zone (mollusc and crustaceans). In addition, since salt mainly comes from the sea, we assumed the concentrations for the pelagic zone also apply to MP in salt.

For the MPs found in air, we acquired concentration data on particulate matter (i.e. total suspended particulates, PM$_{2.5}$, PM$_{10}$) to use as proxies for the chemical concentrations on plastic. This is a fair representation as suspended MPs are part of particulate matter and equilibration between the various components of airborne particulate matter can be assumed.

Finally, as for the MPs in drinking water, beer and milk, we assumed that the chemical concentrations in the MPs are equivalent to that in the plastic packaging. This is partly because MP found in these media can be attributed to the packaging and also the manufacturing process.[11,12] While some chemicals are added as additives such as DEHP, plastic packaging can also contain residues from substances used during the manufacturing process (non-intentionally added substances). Therefore, it is not surprising that plastic packaging may contain traces of

PCBs, PAHs and heavy metals such as lead.[54] An exception is for higher molecular weight PAHs such as BaP, which has not yet been detected in polymer packaging. Li et al.[55] suggested that this may be due to the more complex reaction pathway for such PAHs. Therefore, for BaP, we assumed that the concentration is negligible in the MPs from packaging.

The collected data used for this part of the study and other additional notes on assumptions are accessible in the data depository (Data S5). Fitted or assumed distribution functions for the chemical concentrations are also shown in Table S8.

Supplementary text

Comparison of particle characteristics between food and air

The mass per particle distribution in food is significantly different from that found in air ($p<0.01$; Kruskal-Wallis). MP particles found in air had a narrower mass distribution varying across 5 orders of magnitude while in food, the mass per particle ranged across more than 10 orders of magnitude. Our results also show that the shape distributions (defined by the height : length and width : length ratios; Figures S2A-D) differ for food and air. In the atmosphere, the particles mainly consisted of fibre, fragment and bead shapes which may be a result of textiles or wear-and-tear and UV-degradation of plastic products[56], whereas for food, there was more variation in the particle shapes, including sheet and foam. Unlike the particles found in food which had 15 different polymer types, there were only 5 polymer types found in atmospheric suspension which are commonly used for textiles (Figures S2E and S2F). This verifies that the source of MP in the air is mainly textile-based.
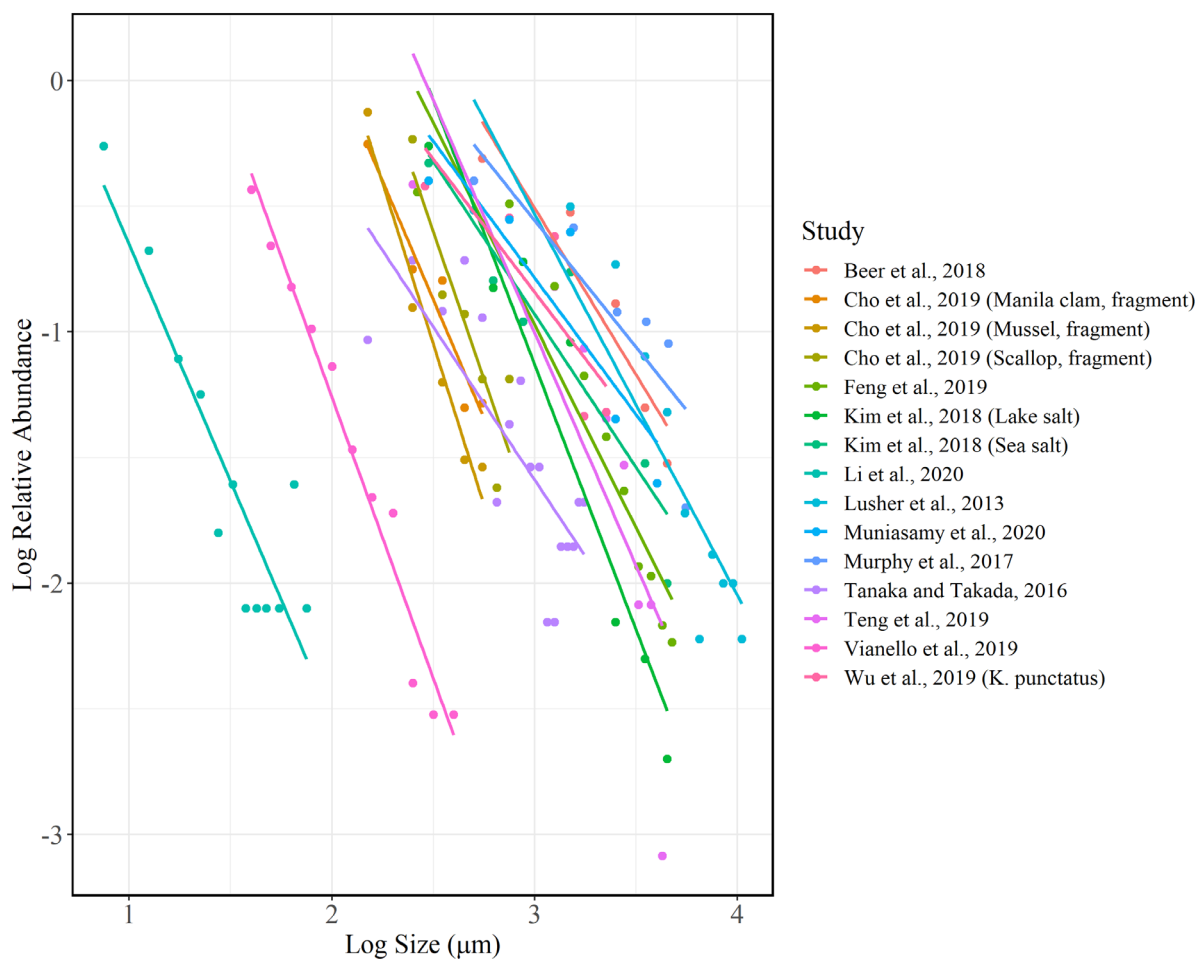
Figure S1. Relative abundance of microplastics vs particle sizes. The fitted trend lines $log(y) = -\alpha \cdot log(x) + C$ for each dataset are displayed.
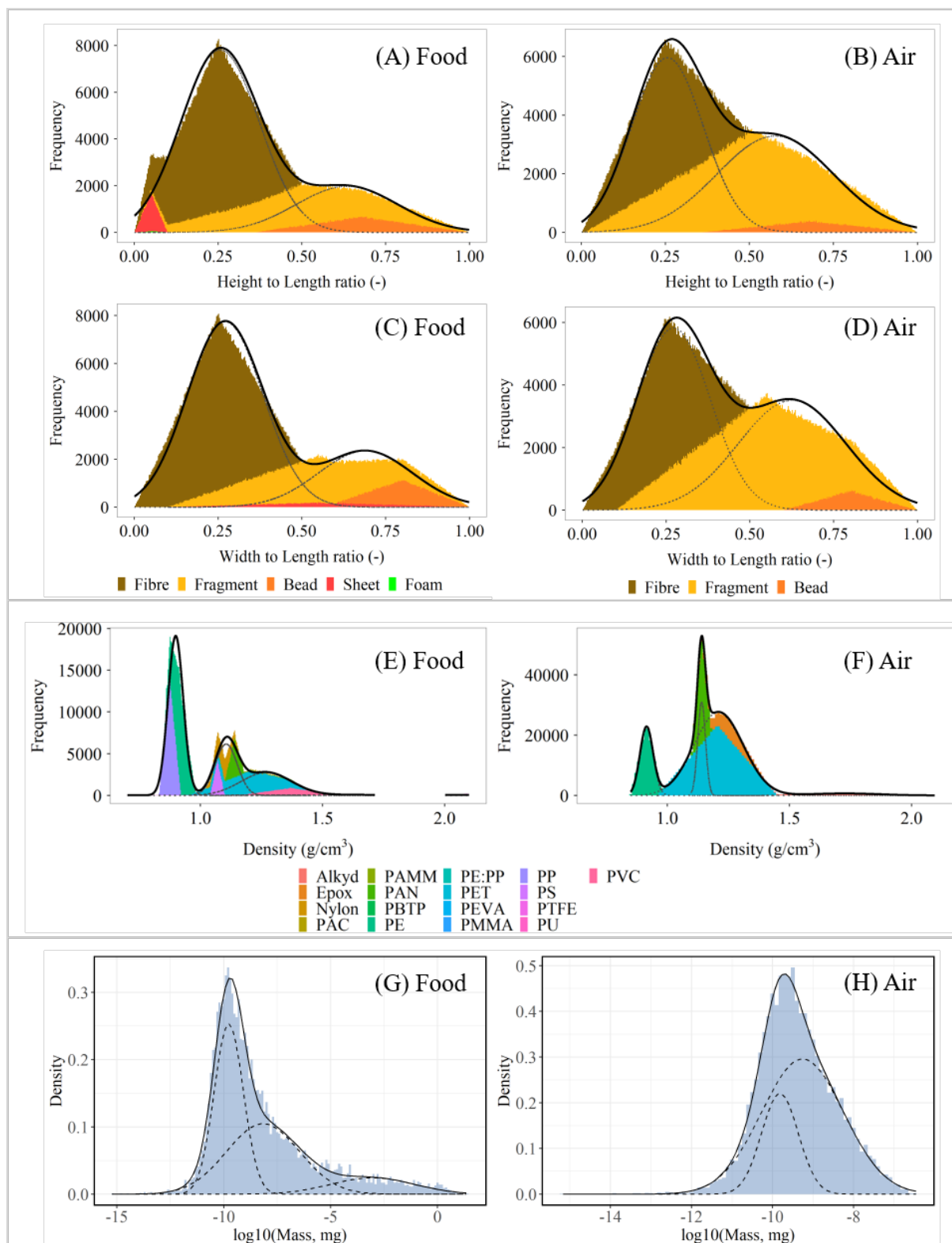
Figure S2. Distributions of particle characteristics from MC simulations (1 000 000 iterations). **(A)** and **(B)** Width to length ratios for food and air. **(C)** and **(D)** Height to length ratios for food and air. **(E)** and **(F)** Density for particles in food and air. **(G)** and **(H)** Mass per particle distributions for food (1-5000 μm) and air (1-10 μm).
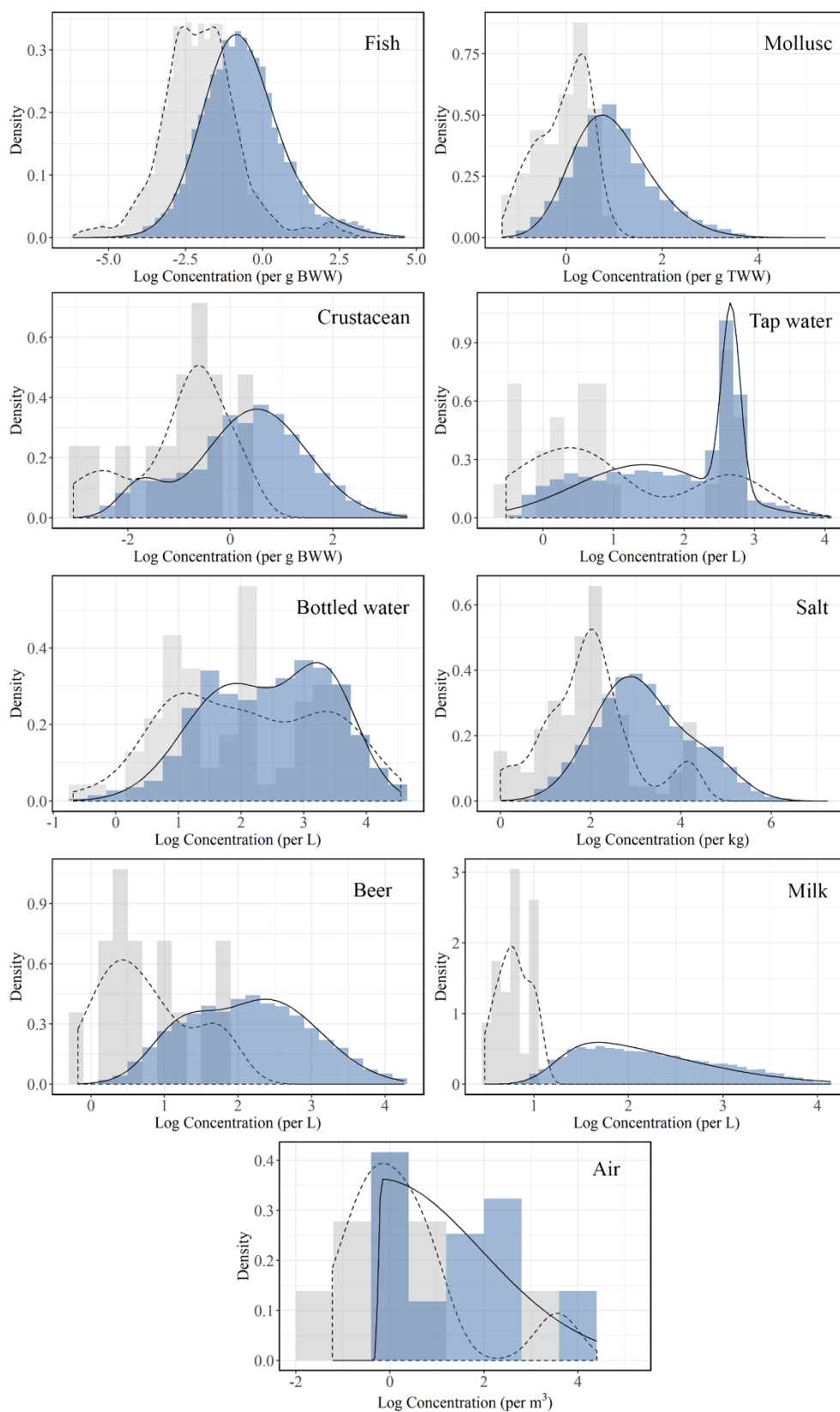
Figure S3. MP exposure number concentrations (logarithmic) in different media and fitted distributions (solid lines). Blue barfills are based on size realigned data (1-5000 μm for food and 1-10 μm for air). Grey barfills are based on the non-size realigned data with the density curve (dotted lines).
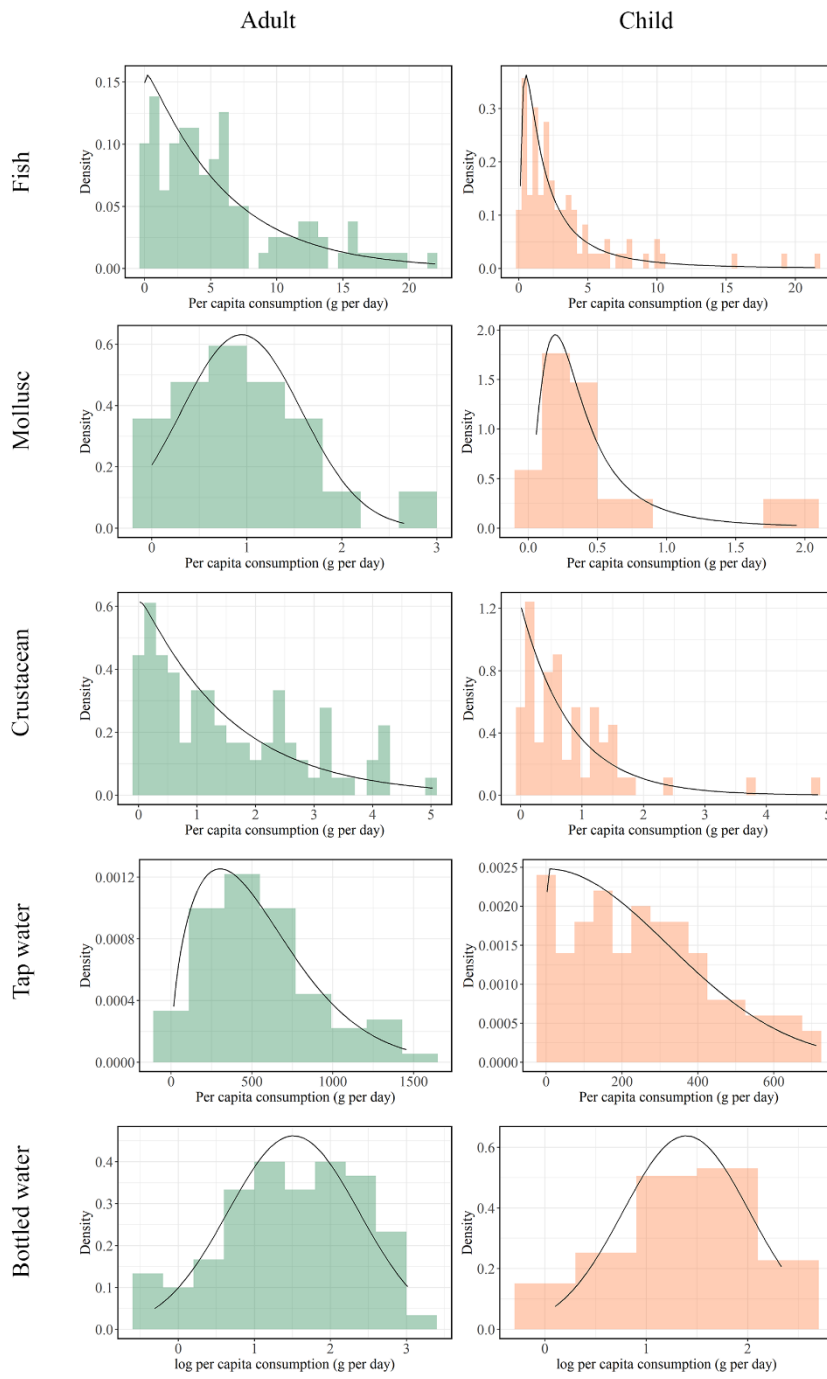
Figure S4. Ingestion rates of food and inhalation rates for adult (green) and child (orange). Ingestion rates for bottled water are on the logarithmic scale. Ingestion rates for beer only applies to adult (blue). The solid lines are the fitted distributions.
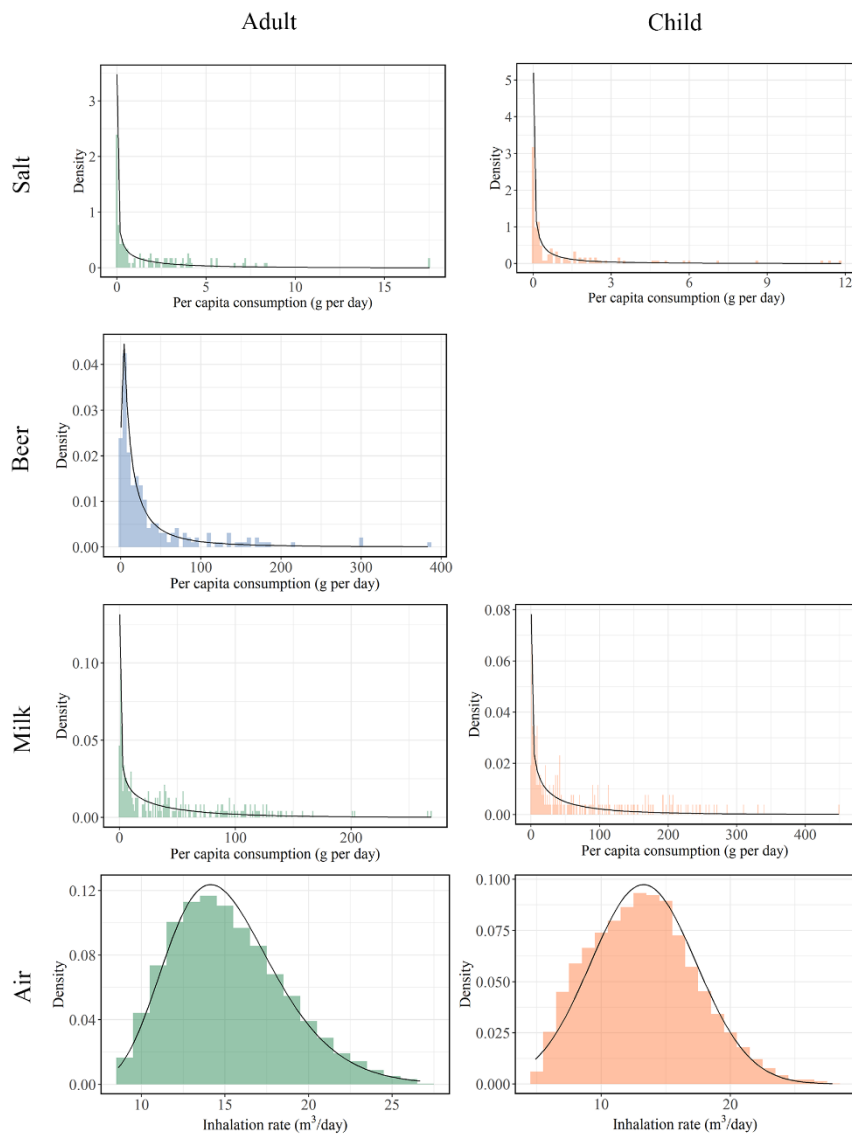
Figure S4. (*continued*)
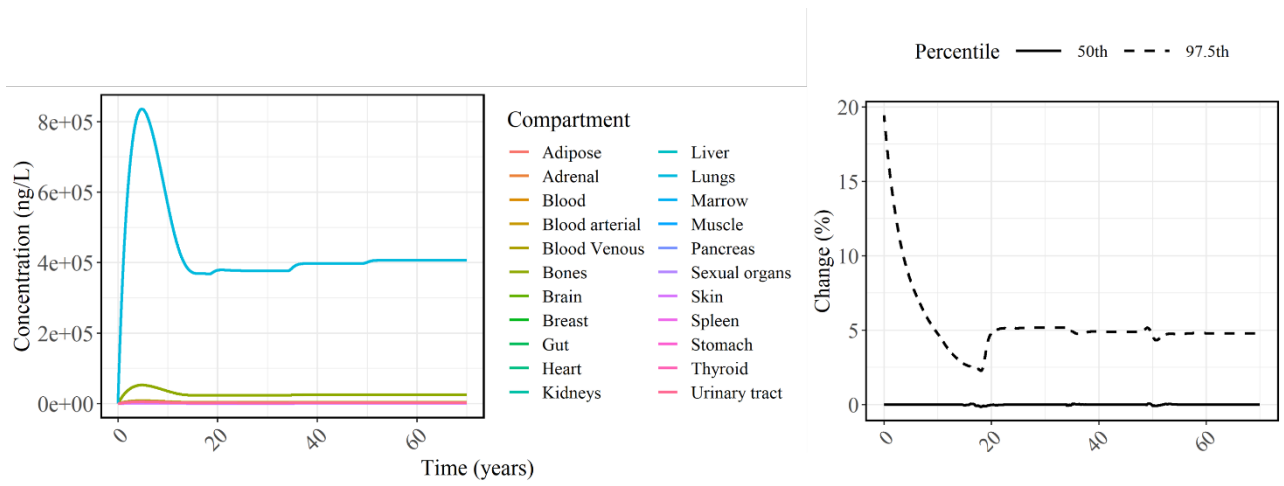
Figure S5. Chemical bioaccumulation of lead in different organs from dietary intake and inhalation in humans over 70 years with PBPK modelling in MERLIN Expo V3.0 (left). Percentage change of lead in adipose tissues as a result of additional chemical exposure via MP (right).

Table S1. Biliary excretion rates (k_{tis}) for human. The rate constants for rat and mouse from Ogawara et al.[57] and Li et al.[58] were rescaled for human with a correction factor of 2.5 which is based on the ratio from the biliary excretion rates of rat:human from Bachler et al.[59].

Material	Size (nm)	Route of exposure	Organism	k_{tis} (min^{-1})	Reference
Polystyrene	50	Intravenous	Rat	8.301	Ogawara et al. [57]
Polystyrene	500	Intravenous	Rat	8.001	Ogawara et al. [57]
Silver NP	15-150	Dermal, oral, inhalation	Human	5.098	Bachler et al. [59]
Poly(lactic-co-glycolic) acid	133.5	Intravenous	Mouse	0.0672	Li et al. [58]
Poly(lactic-co-glycolic) acid	114.8	Intravenous	Mouse	0.672	Li et al. [58]
Poly(lactic-co-glycolic) acid	97.4	Intravenous	Mouse	0.144	Li et al. [58]
Poly(lactic-co-glycolic) acid	79	Intravenous	Mouse	0.557	Li et al. [58]
Poly(lactic-co-glycolic) acid	67	Intravenous	Mouse	0.614	Li et al. [58]
Poly(lactic-co-glycolic) acid	57.5	Intravenous	Mouse	0.394	Li et al. [58]
			No excretion	0	day^{-1}
			Minimum	0.0672	day^{-1}
			Median	0.614	day^{-1}
			Maximum	8.30	day^{-1}

Table S2. Search terms/strings for each food type in FOSCOLLAB

Food type	Search Strings
Fish	Fish (meat); Freshwater fish; Marine fish; Miscellaneous (misc.) coastal marine fishes; Misc. demersal marine fishes; Misc. freshwater fishes; Misc. pelagic marine fishes
Mollusc	Molluscs; Freshwater molluscs; Misc. marine molluscs
Crustacean	Crustaceans; Freshwater shrimps or prawns; Shrimps and prawns; Shrimps; common, White shrimp; Freshwater crayfishes
Tap Water	Tap water; Filtered tap water
Bottled Water	Bottled drinking water; Bottled water; Carbonated bottled drinking water; Flavoured bottled water; Fortified bottled water; Still bottled drinking water
Salt	Salt; Salt, flavoured; Salt, iodised; Salt, iodised and fluoridated; Salt, low Sodium; Sea salt
Beer	Beer; Beer and beer-like beverage; Ale beer; Lager beer; Beer, strong; Beer, regular; Beer, light; Beer, alcohol-free; Pale ale beer; Dark ale beer; Stout beer; Wheat beer; Beer-like beverages; Low malt beers
Milk	Milk; cow milk; cow milk, natural high fat; cow milk, semi skimmed (half fat); cow milk, skimmed (low fat); cow milk, whole

Table S3. Minimum and maximum inhalation rates defined for this study based on Allan and Richardson[21] and Stifelman[22].

Age category	Min inhalation rate (m^3/day)	Max inhalation rate (m^3/day)
Toddlers (7 months–4 years)	4.9	16.1
Children (5 – 11 years)	8.8	23.3
Teenagers (12 – 19 years)	9.5	27.9
Adults (20 – 59 years)	9.7	26.7
Seniors (>60 years)	8.6	24.1

Table S4. Coefficients of fitted linear regressions of log (relative abundance) against log (size). C is the intercept and α is the slope of the regression. SE is the standard error of the parameters and model.

Study	C	SE	α	SE	R^2	Adj. R^2	SE
Food compartment							
Beer et al., 2018	3.47	0.91	1.33	0.28	0.89	0.85	0.2
Cho et al., 2019 (Manila clam fragment)	3.85	0.74	1.89	0.29	0.93	0.91	0.13
Cho et al., 2019 (Mussel fragment)	5.36	0.69	2.56	0.27	0.97	0.96	0.12
Cho et al., 2019 (Scallop fragment)	5.25	1.53	2.34	0.57	0.81	0.76	0.23
Feng et al., 2019	3.86	0.69	1.61	0.21	0.88	0.87	0.25
Kim et al., 2018 (Lake salt)	5.19	0.89	2.11	0.28	0.92	0.9	0.3
Kim et al., 2018 (Sea salt)	2.72	0.68	1.22	0.22	0.86	0.84	0.23
Lusher et al., 2013	4.02	0.85	1.52	0.23	0.82	0.8	0.3
Muniasamy et al., 2020	2.48	0.97	1.09	0.31	0.8	0.74	0.27
Murphy et al., 2017	2.47	1.00	1.01	0.29	0.74	0.68	0.25
Tanaka and Takada, 2016	2.06	0.69	1.22	0.24	0.63	0.61	0.29
Teng et al., 2019	4.55	1.41	1.85	0.43	0.72	0.68	0.49
Wu et al., 2019 (*K. punctatus*)	2.34	1.16	1.06	0.38	0.72	0.62	0.27
Air compartment							
Li et al., 2020 (Air)	1.24	0.42	1.89	0.28	0.82	0.8	0.28
Vianello et al., 2019 (Air)	3.22	0.27	2.24	0.13	0.97	0.97	0.13

Table S5. MP concentrations in muscle and gut per g BWW (body wet weight) and the ratio between muscle and gut concentrations (CF_{mg}). Data adapted from Abbasi et al.[27] and Barboza et al.[28].

Species	N	Total weight of N species (g)	MP conc in muscle (#/g BWW)	MP conc in gut (#/g BWW)	Ratio (muscle:gut)	Reference
Sillago sihama	17	972.4	0.055	0.015	3.533	Abbasi et al., 2018
Platycephalus indicus	12	441.6	0.109	0.057	1.921	Abbasi et al., 2018
Saurida tumbil	4	144.4	0.083	0.069	1.200	Abbasi et al., 2018
Cynoglossus abbreviatus	11	833.8	0.031	0.037	0.838	Abbasi et al., 2018
Dicentrarchus labrax	50	17150	0.001	0.004	0.269	Barboza et al., 2020
Trachurus trachurus	50	11400	0.003	0.004	0.673	Barboza et al., 2020
Scomber colias	50	17200	0.002	0.003	0.508	Barboza et al., 2020
				Average (±SD)	1.28 (±1.13)	
				Minimum	0.27	
				Maximum	3.53	

Table S6. Probability density functions for exposure parameters used to perform probabilistic exposure assessment to MPs through dietary and inhalation intake

Parameter	Variable	Distribution	Units	Parameters	Percentile[#]
Exposure media (logarithmic concentrations)					
Fish	Cf	Bimodal[§]	#/g BWW	$\mu 1 = -0.94$ $\sigma 1 = 1.06$ $\lambda 1 = 0.71$ $\mu 2 = 0.09$ $\sigma 2 = 1.69$ $\lambda 2 = 0.29$	$50^{th} = -0.73$ $95^{th} = 1.79$
Mollusc	Cm	Skew-t[^]	#/g TWW	$x_i = 0.12$ $\omega = 1.19$ $\alpha = 2.03$	$50^{th} = 0.91$ $95^{th} = 2.63$
Crustacean	Ccr	Bimodal[§]	#/g BWW	$\mu 1 = -1.76$ $\sigma 1 = 0.40$ $\lambda 1 = 0.11$ $\mu 2 = 0.52$ $\sigma 2 = 0.99$ $\lambda 2 = 0.89$	$50^{th} = 0.38$ $95^{th} = 2.11$
Tap water	Ctw	Bimodal[§]	#/L	$\mu 1 = 1.44$ $\sigma 1 = 0.99$ $\lambda 1 = 0.68$ $\mu 2 = 2.66$ $\sigma 2 = 0.13$ $\lambda 2 = 0.32$	$50^{th} = 2.10$ $95^{th} = 3.02$
Bottled water	Cbw	Bimodal[§]	#/L	$\mu 1 = 1.83$ $\sigma 1 = 0.78$ $\lambda 1 = 0.59$ $\mu 2 = 3.34$ $\sigma 2 = 0.53$ $\lambda 2 = 0.41$	$50^{th} = 2.53$ $95^{th} = 3.97$
Salt	Cs	Bimodal[§]	#/kg	$\mu 1 = 2.84$ $\sigma 1 = 0.85$ $\lambda 1 = 0.80$ $\mu 2 = 4.62$ $\sigma 2 = 0.68$ $\lambda 2 = 0.20$	$50^{th} = 3.11$ $95^{th} = 5.08$
Beer	Cb	Bimodal[§]	#/L	$\mu 1 = 1.19$ $\sigma 1 = 0.42$ $\lambda 1 = 0.23$ $\mu 2 = 2.41$ $\sigma 2 = 0.73$ $\lambda 2 = 0.77$	$50^{th} = 2.12$ $95^{th} = 3.55$

Table S6. (*continued*)

Parameter	Variable	Distribution	Units	Parameters	Percentile[#]
Milk	Cmk	Skew-normal^	#/L	$x_i = 1.23$ $\omega = 1.22$ $\alpha = 5.06$	$50^{th} = 2.12$ $95^{th} = 3.51$
Air	Ca	Skew-normal^	#/m³	$x_i = -0.25$ $\omega = 2.20$ $\alpha = 67.8$	$50^{th} = 1.56$ $95^{th} = 4.28$
Physiological data					
Ingestion rate, fish, adult	Irfadult	Weibull*	g/capita/day	$k = 1.02$ $\lambda = 5.89$	$50^{th} = 4.33$ $95^{th} = 16.41$
Ingestion rate, fish, child	Irfchild	Lognormal	g/capita/day	meanlog = 0.61 sdlog = 1.15	$50^{th} = 2.08$ $95^{th} = 9.94$
Ingestion rate, mollusc, adult	Irmadult	Normal	g/capita/day	$\mu = 0.945$ $\sigma = 0.632$	$50^{th} = 0.86$ $95^{th} = 1.85$
Ingestion rate, mollusc, child	Irmchild	Log-log‡	g/capita/day	$\beta = 2.014$ $\alpha = 0.333$	$50^{th} = 0.31$ $95^{th} = 1.76$
Ingestion rate, crustacean, adult	Ircadult	Weibull*	g/capita/day	$k = 1.02$ $\lambda = 1.52$	$50^{th} = 1.16$ $95^{th} = 4.13$
Ingestion rate, crustacean, child	Ircchild	Exponential†	g/capita/day	$\lambda = 1.22$	$50^{th} = 0.58$ $95^{th} = 1.85$
Ingestion rate, tapwater, adult	Irtwadult	Weibull*	g/capita/day	$k = 1.54$ $\lambda = 598.8$	$50^{th} = 502.1$ $95^{th} = 1255.2$
Ingestion rate, tapwater, child	Irtwchild	Skew-normal^	g/capita/day	$x_i = 0.104$ $\omega = 321.5$ $\alpha = 183.4$	$50^{th} = 241.5$ $95^{th} = 619.7$
Ingestion rate, botwater, adult (logarithmic)	Irbwadult	Normal	g/capita/day	$\mu = 1.51$ $\sigma = 0.864$	$50^{th} = 1.57$ $95^{th} = 2.64$
Ingestion rate, botwater, child (logarithmic)	Irbwchild	Normal	g/capita/day	$\mu = 1.39$ $\sigma = 0.626$	$50^{th} = 1.41$ $95^{th} = 2.28$
Ingestion rate, salt, adult	Irsadult	Gamma[#]	g/capita/day	$k = 0.429$ $\theta = 0.217$	$50^{th} = 0.57$ $95^{th} = 7.25$
Ingestion rate, salt, child	Irschild	Weibull*	g/capita/day	$k = 0.526$ $\lambda = 0.660$	$50^{th} = 0.24$ $95^{th} = 5.69$
Ingestion rate, beer	Irb	Lognormal	g/capita/day	meanlog = 2.71 sdlog = 1.49	$50^{th} = 16.6$ $95^{th} = 161.7$
Ingestion rate, milk, adult	Irmkadult	Gamma[#]	g/capita/day	$k = 0.605$ $\theta = 0.014$	$50^{th} = 26.5$ $95^{th} = 129.6$
Ingestion rate, milk, child	Irmkchild	Weibull*	g/capita/day	$k = 0.688$ $\lambda = 51.2$	$50^{th} = 27.9$ $95^{th} = 236.4$

Table S6. (*continued***)**

Parameter	Variable	Distribution	Units	Parameters	Percentile[#]
Inhalation rate, adult	InRadult	Lognormal	m^3/capita/day	meanlog = 2.70 sdlog = 0.22	50th = 14.8 95th = 21.6
Inhalation rate, child	InRchild	Normal	m^3/capita/day	μ = 13.23 σ = 4.07	50th = 13.1 95th = 20.4
Stool frequency, adult	$k_{loss,\ adult}$	Triangular	day^{-1}	min = 0.4 max = 3	
Stool frequency, child	$k_{loss,\ child}$	Triangular	day^{-1}	min = 0.8 max = 3	
Stool mass, adult	$M_{stool,\ adult}$	Triangular	g/capita/day	min = 51 max = 796	
Stool mass, child	$M_{stool,\ child}$	Triangular	g/capita/day	min = 51 max = 699	

[§]μ is the mean, σ is the standard deviation and λ is the probability of the bimodal distribution functions

[^]x_i is the location parameter, ω is the scale parameter, α is the shape parameter for skew-normal, skew-*t* and skew-cauchy distribution.

[*]*k* is the shape parameter and λ is the scale parameter for a Weibull distribution.

[#]*k* is the shape parameter and θ is the rate parameter for a gamma distribution.

[†]λ is the rate constant for an exponential distribution.

[‡]β is the shape parameter and α is the scale parameter for a log-logistic distribution.

BWW: Body wet weight

TWW: Tissue wet weight

Table S7. Parameters of fitted distributions for shape, density and mass of MP particles for number to mass concentrations conversion.

Media	Property	Fitted distribution	Probability	μ	σ
Food	Height:Length	Bimodal	0.749	0.255	0.116
			0.251	0.632	0.153
Food	Width:Length	Bimodal	0.728	0.271	0.113
			0.272	0.690	0.140
Air	Height:Length	Bimodal	0.528	0.256	0.107
			0.472	0.577	0.173
	Width:Length	Bimodal	0.533	0.272	0.110
			0.467	0.626	0.161
Food	Density	4-modal	0.031	1.687	0.564
			0.234	1.105	0.045
			0.237	1.268	0.104
			0.498	0.898	0.031
Air	Density	4-modal	0.024	1.726	0.144
			0.124	1.140	0.016
			0.151	0.915	0.027
			0.700	1.209	0.101
Food	Mass	3-modal	0.45	-8.17	1.71
			0.43	-9.77	0.68
			0.12	-3.04	1.96
Air	Mass	Bimodal	0.75	-9.26	1.01
			0.25	-9.82	0.45

Table S8. Probability density functions for chemical concentrations on plastic of each media category. Goodness-of-fit analysis was not carried out for these datasets due to low sample size. Distributions with the best fit were evaluated visually.

Chemical	Media category	Distribution	Units	Parameters
PCB126	Pelagic	Exponential[†]	ng/g lipid	λ=0.225
	Littoral	Exponential[†]	ng/g lipid	λ=17.48
	Packaging	Triangle	µg/kg	min=0 max=7.9
	Air	Log-logistic[‡]	pg/m^3	β=1.12 α=0.155
Lead	Pelagic	Lognormal	mg/kg ww	meanlog=-2.17 sdlog=2.12
	Littoral	Lognormal	mg/kg ww	meanlog=-1.78 sdlog=1.32
	Packaging	Lognormal	mg/kg	meanlog=4.00 sdlog=4.00
	Air	Lognormal	ng/m^3	meanlog=4.22 sdlog=1.88
DEHP	Pelagic	Lognormal	ng/g lipid	meanlog=8.83 sdlog=1.60
	Littoral	Triangle	ng/g lipid	min=0 max=5284
	Packaging	Log-logistic[‡]	µg/kg	β=0.59 α=89261.05
	Air	Log-logistic[‡]	pg/m^3	β=1.42 α=35594.55
BaP	Pelagic	Lognormal	ng/g lipid	meanlog=6.09 sdlog=3.55
	Littoral	Exponential	ng/g lipid[†]	λ=0.023
	Air	Log-logistic[‡]	pg/m^3	β=1.55 α=146.09

[†]λ is the rate constant for an exponential distribution.

[‡]β is the shape parameter and α is the scale parameter for a log-logistic distribution.

Table S9. Percentiles of MP number concentration in gut, tissue and stools for each scenario of biliary excretion. Scenarios: no biliary excretion ($k_{tis} = 0$ d^{-1}); minimum ($k_{tis} = 0.067$ d^{-1}), median ($k_{tis} = 0.61$ d^{-1}); maximum ($k_{tis} = 8.30$ d^{-1}).

Age category	Percentile (%)	Zero	Minimum	Median	Maximum
Concentration in gut (log #/capita); $p<0.05$ between children & adults (Kruskal-Wallis)					
Child	2.50	1.27	1.27	1.29	1.29
	5	1.42	1.43	1.44	1.44
	25	2.00	2.00	2.02	2.02
	50	2.48	2.48	2.50	2.50
	75	3.16	3.16	3.21	3.21
	95	4.77	4.78	4.93	4.93
	97.5	5.45	5.46	5.55	5.55
Adult	2.50	1.53	1.54	1.56	1.56
	5	1.70	1.70	1.71	1.71
	25	2.28	2.28	2.29	2.29
	50	2.74	2.74	2.74	2.74
	75	3.38	3.38	3.41	3.41
	95	4.93	4.93	5.05	5.05
	97.5	5.55	5.55	5.69	5.69
Concentration in tissue (log #/capita); $p<0.05$ between children & adults (Kruskal-Wallis)					
Child	2.50	2.72	0.12	-0.83	-1.96
	5	2.85	0.26	-0.68	-1.81
	25	3.42	0.83	-0.11	-1.24
	50	3.92	1.32	0.37	-0.76
	75	4.64	2.04	1.14	0.00
	95	6.28	3.68	2.86	1.73
	97.5	6.92	4.33	3.49	2.36
Adult	2.50	3.56	0.33	-0.63	-1.76
	5	3.72	0.48	-0.46	-1.59
	25	4.25	1.05	0.09	-1.04
	50	4.70	1.51	0.55	-0.58
	75	5.37	2.17	1.25	0.12
	95	6.97	3.75	2.92	1.79
	97.5	7.61	4.41	3.57	2.44
Concentration in stool (#/g stool/capita); $p<0.05$ between children & adults (Kruskal-Wallis)					
Child	2.50	0.084	0.083	0.084	0.087
	5	0.124	0.124	0.128	0.127
	25	0.510	0.513	0.530	0.517
	50	1.657	1.634	1.715	1.731
	75	8.188	8.197	9.166	8.935
	95	328.56	343.5	479.4	482.0
	97.5	1578.3	1599.1	1935.6	2032.7
Adult	2.50	0.12	0.12	0.12	0.12
	5	0.17	0.18	0.18	0.18
	25	0.74	0.73	0.75	0.77
	50	2.31	2.36	2.38	2.39
	75	10.5	10.4	12.2	11.6
	95	372.1	363.0	490.7	487.2
	97.5	1617.3	1627.1	2140.2	2138.4

Table S10. Percentiles of MP mass concentration in gut and tissue for each scenario of biliary excretion. Scenarios: no biliary excretion (k_{tis} = 0 d^{-1}); minimum (k_{tis} = 0.067 d^{-1}), median (k_{tis} = 0.61 d^{-1}); maximum (k_{tis} = 8.30 d^{-1}).

Age category	Percentile (%)	Zero	Minimum	Median	Maximum
Concentration in gut (mg MP/capita); $p<0.05$ between children & adults (Kruskal-Wallis)					
Child	2.50	3.14E-09	3.13E-09	3.13E-09	3.13E-09
	5	6.38E-09	6.15E-09	6.44E-09	6.25E-09
	25	7.05E-08	7.31E-08	7.24E-08	7.11E-08
	50	8.05E-07	7.98E-07	8.77E-07	8.52E-07
	75	2.69E-05	2.72E-05	2.58E-05	2.88E-05
	95	3.12E-01	1.96E-01	1.86E-01	2.18E-01
	97.5	4.67	2.68	3.26	2.97
Adult	2.50	5.32E-09	5.67E-09	5.38E-09	5.25E-09
	5	9.76E-09	1.07E-08	1.11E-08	1.04E-08
	25	1.28E-07	1.26E-07	1.33E-07	1.34E-07
	50	1.42E-06	1.41E-06	1.55E-06	1.59E-06
	75	5.01E-05	4.64E-05	5.97E-05	4.89E-05
	95	5.79E-01	3.45E-01	4.62E-01	5.88E-01
	97.5	7.29	5.17	8.21	7.21
Concentration in tissue (mg MP/capita); $p<0.05$ between children & adults (Kruskal-Wallis)					
Child	2.50	6.21E-08	1.72E-10	1.85E-11	1.33E-12
	5	1.17E-07	3.07E-10	3.47E-11	2.65E-12
	25	9.99E-07	2.82E-09	3.15E-10	2.24E-11
	50	6.36E-06	1.73E-08	1.95E-09	1.43E-10
	75	5.05E-05	1.38E-07	1.55E-08	1.17E-09
	95	2.31E-03	5.55E-06	7.02E-07	5.41E-08
	97.5	8.87E-03	2.15E-05	3.70E-06	2.48E-07
Adult	2.50	4.47E-07	2.61E-10	2.69E-11	2.24E-12
	5	8.15E-07	4.66E-10	5.23E-11	4.16E-12
	25	7.08E-06	4.26E-09	4.71E-10	3.70E-11
	50	4.07E-05	2.53E-08	2.89E-09	2.22E-10
	75	2.82E-04	1.95E-07	2.32E-08	1.76E-09
	95	9.85E-03	6.22E-06	9.00E-07	6.89E-08
	97.5	4.81E-02	2.61E-05	3.62E-06	2.85E-07

References

(1)   Mühlschlegel, P.; Hauk, A.; Walter, U.; Sieber, R. Lack of Evidence for Microplastic Contamination in Honey. *Food Addit. Contam. - Part A Chem. Anal. Control. Expo. Risk Assess.* **2017**, *34* (11), 1982–1989. https://doi.org/10.1080/19440049.2017.1347281.

(2)   Li, Q.; Feng, Z.; Zhang, T.; Ma, C.; Shi, H. Microplastics in the Commercial Seaweed Nori. *J. Hazard. Mater.* **2020**, *388* (October 2019), 122060. https://doi.org/10.1016/j.jhazmat.2020.122060.

(3)   Karami, A.; Golieskardi, A.; Ho, Y. Bin; Larat, V.; Salamatinia, B. Microplastics in Eviscerated Flesh and Excised Organs of Dried Fish. *Sci. Rep.* **2017**, *7* (1), 1–9. https://doi.org/10.1038/s41598-017-05828-6.

(4)   Huerta Lwanga, E.; Mendoza Vega, J.; Ku Quej, V.; Chi, J. de los A.; Sanchez del Cid, L.; Chi, C.; Escalona Segura, G.; Gertsen, H.; Salánki, T.; van der Ploeg, M.; Koelmans, A. A.; Geissen, V. Field Evidence for Transfer of Plastic Debris along a Terrestrial Food Chain. *Sci. Rep.* **2017**, *7* (1), 1–7. https://doi.org/10.1038/s41598-017-14588-2.

(5)   Hermsen, E.; Mintenig, S.; Besseling, E.; Koelmans, A. A. Quality Criteria for the Analysis of Microplastic in Biota Samples. Critical Review. *Environ. Sci. Technol.* **2018**. https://doi.org/10.1021/acs.est.8b01611.

(6)   Ferdouse, F.; Løvstad Holdt, S.; Smith, R.; Murúa, P.; Yang, Z. The Global Status of Seaweed Production, Trade and Utilization. *FAO Globefish Res. Program.* **2018**.

(7)   Koelmans, A. A.; Mohamed Nor, N. H.; Hermsen, E.; Kooi, M.; Mintenig, S. M.; De France, J. Microplastics in Freshwaters and Drinking Water: Critical Review and Assessment of Data Quality. *Water Research.* 2019. https://doi.org/10.1016/j.watres.2019.02.054.

(8)   Winkler, A.; Santo, N.; Ortenzi, M. A.; Bolzoni, E.; Bacchetta, R.; Tremolada, P. Does Mechanical Stress Cause Microplastic Release from Plastic Water Bottles? *Water Res.* **2019**. https://doi.org/10.1016/j.watres.2019.115082.

(9)   Zhang, M.; Li, J.; Ding, H.; Ding, J.; Jiang, F.; Ding, N. X.; Sun, C. Distribution Characteristics and Influencing Factors of Microplastics in Urban Tap Water and Water Sources in Qingdao, China. *Anal. Lett.* **2019**, *0* (0), 1–16. https://doi.org/10.1080/00032719.2019.1705476.

(10)   Kankanige, D.; Babel, S. Smaller-Sized Micro-Plastics (MPs) Contamination in Single-Use PET-Bottled Water in Thailand. *Sci. Total Environ.* **2020**. https://doi.org/10.1016/j.scitotenv.2020.137232.

(11)   Kutralam-Muniasamy, G.; Pérez-Guevara, F.; Elizalde-Martínez, I.; Shruti, V. C. Branded Milks – Are They Immune from Microplastics Contamination? *Sci. Total Environ.* **2020**, *714*. https://doi.org/10.1016/j.scitotenv.2020.136823.

(12)   Kosuth, M.; Mason, S. A.; Wattenberg, E. V. Anthropogenic Contamination of Tap Water, Beer, and Sea Salt. *PLoS One* **2018**, *13* (4). https://doi.org/10.1371/journal.pone.0194970.

(13)   Liebezeit, G.; Liebezeit, E. Synthetic Particles as Contaminants in German Beers. *Food Addit. Contam. - Part A Chem. Anal. Control. Expo. Risk Assess.* **2014**, *31* (9), 1574–1578. https://doi.org/10.1080/19440049.2014.945099.

(14)   Kennedy, N. J.; Hinds, W. C. Inhalability of Large Solid Particles. *J. Aerosol Sci.* **2002**. https://doi.org/10.1016/S0021-8502(01)00168-9.

(15)   Froese, R.; Pauly, D. Fishbase. World Wide Web electronic publication.

(16)   Hartmann, N. B.; Hüffer, T.; Thompson, R. C.; Hassellöv, M.; Verschoor, A.; Daugaard, A. E.; Rist, S.; Karlsson, T.; Brennholt, N.; Cole, M.; Herrling, M. P.; Hess, M. C.; Ivleva, N. P.; Lusher, A. L.; Wagner, M. Are We Speaking the Same Language? Recommendations for a Definition and Categorization Framework for Plastic Debris. *Environ. Sci. Technol.* **2019**. https://doi.org/10.1021/acs.est.8b05297.

(17)   Koelmans, A. A.; Redondo-Hasselerharm, P. E.; Mohamed Nor, N. H.; Kooi, M. Solving the Non-Alignment of Methods and Approaches Used in Microplastic Research in Order to Consistently Characterize Risk. *Environ. Sci. Technol.* **2020**.

(18)   SAPEA. A Scientific Perspective on Microplastics in Nature and Society | SAPEA. *Evid. Rev. Rep.* **2019**. https://doi.org/10.26356/microplastics.

(19)   Mintenig, S. M.; Bäuerlein, P. S.; Koelmans, A. A.; Dekker, S. C.; Van Wezel, A. P. Closing the Gap between Small and Smaller: Towards a Framework to Analyse Nano- and Microplastics in Aqueous Environmental Samples. *Environ. Sci. Nano* **2018**. https://doi.org/10.1039/c8en00186c.

(20)   Lenz, R.; Enders, K.; Stedmon, C. A.; MacKenzie, D. M. A.; Nielsen, T. G. A Critical Assessment of Visual Identification of Marine Microplastic Using Raman Spectroscopy for Analysis Improvement. *Mar. Pollut. Bull.* **2015**. https://doi.org/10.1016/j.marpolbul.2015.09.026.

(21)   Allan, M.; Richardson, G. M. Human and Ecological Risk Assessment : An International Probability Density Functions Describing 24-Hour Inhalation Rates For Use in Human Health Risk Assessments Probability Density Functions Describing 24-Hour Inhalation Rates For Use in Human Health Ri. **2010**, *7039*. https://doi.org/10.1080/10807039891284389.

(22)   Stifelman, M. Using Doubly-Labeled Water Measurements of Human Energy Expenditure to Estimate Inhalation Rates. *Sci. Total Environ.* **2007**, *373* (2–3), 585–590. https://doi.org/10.1016/j.scitotenv.2006.11.041.

(23)   USEPA. *EXPOSURE FACTORS HANDBOOK : 2011 EDITION*; 2011. https://doi.org/EPA/600/R-09/052F.

(24)   Kooi, M.; Koelmans, A. A. Simplifying Microplastic via Continuous Probability Distributions for Size, Shape, and Density. *Environ. Sci. Technol. Lett.* **2019**. https://doi.org/10.1021/acs.estlett.9b00379.

(25)   Cózar, A.; Echevarría, F.; González-Gordillo, J. I.; Irigoien, X.; Úbeda, B.; Hernández-León, S.; Palma, Á. T.; Navarro, S.; García-de-Lomas, J.; Ruiz, A.; Fernández-de-Puelles, M. L.; Duarte, C. M. Plastic Debris in the Open Ocean. *Proc. Natl. Acad. Sci. U. S. A.* **2014**. https://doi.org/10.1073/pnas.1314705111.

(26)   EFSA. Presence of Microplastics and Nanoplastics in Food, with Particular Focus on Seafood. *EFSA J.* **2016**, *14* (6). https://doi.org/10.2903/j.efsa.2016.4501.

(27)   Abbasi, S.; Soltani, N.; Keshavarzi, B.; Moore, F.; Turner, A.; Hassanaghaei, M. Microplastics in Different Tissues of Fish and Prawn from the Musa Estuary, Persian Gulf. *Chemosphere* **2018**, *205*, 80–87.

https://doi.org/10.1016/j.chemosphere.2018.04.076.

(28)   Barboza, L. G. A.; Lopes, C.; Oliveira, P.; Bessa, F.; Otero, V.; Henriques, B.; Raimundo, J.; Caetano, M.; Vale, C.; Guilhermino, L. Microplastics in Wild Fish from North East Atlantic Ocean and Its Potential for Causing Neurotoxic Effects, Lipid Oxidative Damage, and Human Health Risks Associated with Ingestion Exposure. *Sci. Total Environ.* **2020**, *717* (xxxx). https://doi.org/10.1016/j.scitotenv.2019.134625.

(29)   Johnson, R. A.; Wichern, D. W. Applied Multivariate Statistical Analysis. Prentice Hall, Englewood Cliffs, NJ. *Appl. Multivar. Stat. Anal. Prentice-Hall, Englewood Cliffs, NJ.* **1992**.

(30)   Granger, C. W. J. Extracting Information from Mega-Panels and High-Frequency Data. *Stat. Neerl.* **1998**, *52* (3), 258–272.

(31)   Benaglia, T.; Chauveau, D.; Hunter, D. R.; Young, D. Mixtools: An R Package for Analyzing Finite Mixture Models. *J. Stat. Softw.* **2009**, *32* (6), 1–29.

(32)   Duis, K.; Coors, A. Microplastics in the Aquatic and Terrestrial Environment: Sources (with a Specific Focus on Personal Care Products), Fate and Effects. *Environmental Sciences Europe.* 2016. https://doi.org/10.1186/s12302-015-0069-y.

(33)   Polymerdatabase.com. Average density of amorphous polymers http://polymerdatabase.com/polymer physics/Polymer Density.html (accessed Aug 5, 2020).

(34)   Scientific polymer products. Density of polymers (by density) https://scientificpolymer.com/density-of-polymers-by-density/ (accessed Aug 5, 2020).

(35)   Omnexus. Density of plastics: Technical properties https://omnexus.specialchem.com/polymer-properties/properties/density (accessed Aug 5, 2020).

(36)   Prospector. Polyurethane (PUR) typical properties generic PUR, unspecified https://plastics.ulprospector.com/generics/45/c/t/polyurethane-pur-properties-processing (accessed Aug 5, 2020).

(37)   Llobet, J. M.; Bocio, A.; Domingo, J. L.; Teixidó, A.; Casas, C.; Müller, L. Levels of Polychlorinated Biphenyls in Foods from Catalonia, Spain: Estimated Dietary Intake. *J. Food Prot.* **2003**. https://doi.org/10.4315/0362-028X-66.3.479.

(38)   Malavolti, M.; Fairweather-Tait, S. J.; Malagoli, C.; Vescovi, L.; Vinceti, M.; Filippini, T. Lead Exposure in an Italian Population: Food Content, Dietary Intake and Risk Assessment. *Food Res. Int.* **2020**, *137*, 109370. https://doi.org/https://doi.org/10.1016/j.foodres.2020.109370.

(39)   Buonanno, G.; Giovinco, G.; Morawska, L.; Stabile, L. Lung Cancer Risk of Airborne Particles for Italian Population. *Environ. Res.* **2015**. https://doi.org/10.1016/j.envres.2015.07.019.

(40)   Heinemeyer, G.; Sommerfeld, C.; Springer, A.; Heiland, A.; Lindtner, O.; Greiner, M.; Heuer, T.; Krems, C.; Conrad, A. Estimation of Dietary Intake of Bis(2-Ethylhexyl)Phthalate (DEHP) by Consumption of Food in the German Population. *Int. J. Hyg. Environ. Health* **2013**. https://doi.org/10.1016/j.ijheh.2013.01.001.

(41)   Fromme, H.; Lahrz, T.; Piloty, M.; Gebhart, H.; Oddoy, A.; Rüden, H. Occurrence of Phthalates and Musk Fragrances in Indoor Air and Dust from Apartments and

Kindergartens in Berlin (Germany). *Indoor Air* **2004**. https://doi.org/10.1111/j.1600-0668.2004.00223.x.

(42) Xie, Z.; Selzer, J.; Ebinghaus, R.; Caba, A.; Ruck, W. Development and Validation of a Method for the Determination of Trace Alkylphenols and Phthalates in the Atmosphere. *Anal. Chim. Acta* **2006**. https://doi.org/10.1016/j.aca.2006.02.027.

(43) Stolzenberg, H.; Kahl, H.; Bergmann, K. E. Körpermaße Bei Kindern Und Jugendlichen in Deutschland. *Bundesgesundheitsblatt. Gesundheitsforschung. Gesundheitsschutz* **2007**. https://doi.org/10.1007/s00103-007-0227-5.

(44) Manz, F.; Johner, S. A.; Wentz, A.; Boeing, H.; Remer, T. Water Balance throughout the Adult Life Span in a German Population. *Br. J. Nutr.* **2012**. https://doi.org/10.1017/S0007114511004776.

(45) Lee, B. M.; Shim, G. A. Dietary Exposure Estimation of Benzo[a]Pyrene and Cancer Risk Assessment. *J. Toxicol. Environ. Heal. - Part A Curr. Issues* **2007**, No. 70, 1391–1394. https://doi.org/10.1080/15287390701434182.

(46) Hong, W. J.; Jia, H.; Ma, W. L.; Sinha, R. K.; Moon, H. B.; Nakata, H.; Minh, N. H.; Chi, K. H.; Li, W. L.; Kannan, K.; Sverko, E.; Li, Y. F. Distribution, Fate, Inhalation Exposure and Lung Cancer Risk of Atmospheric Polycyclic Aromatic Hydrocarbons in Some Asian Countries. *Environ. Sci. Technol.* **2016**. https://doi.org/10.1021/acs.est.6b01090.

(47) Gao, Q.; Ben, Y.; Dong, Z.; Hu, J. Age-Dependent Human Elimination Half-Lives of Dioxin-like Polychlorinated Biphenyls Derived from Biomonitoring Data in the General Population. *Chemosphere* **2019**. https://doi.org/10.1016/j.chemosphere.2019.01.168.

(48) Brochot, C.; Quindroit, P. Modelling the Fate of Chemicals in Humans Using a Lifetime Physiologically Based Pharmacokinetic (PBPK) Model in MERLIN-Expo. In *Handbook of Environmental Chemistry*; 2018. https://doi.org/10.1007/978-3-319-59502-3_10.

(49) Chiang, K. C.; Liao, C. M. Heavy Incense Burning in Temples Promotes Exposure Risk from Airborne PMs and Carcinogenic PAHs. *Sci. Total Environ.* **2006**. https://doi.org/10.1016/j.scitotenv.2006.08.012.

(50) Gentry, P. R.; Clewell, H. J.; Clewell, R.; Campbell, J.; Van Landingham, C.; Shipp, A. M. Challenges in the Application of Quantitative Approaches in Risk Assessment: A Case Study with Di-(2-Ethylhexyl)Phthalate. *Critical Reviews in Toxicology*. 2011. https://doi.org/10.3109/10408444.2011.599366.

(51) Mohamed Nor, N. H.; Koelmans, A. A. Transfer of PCBs from Microplastics under Simulated Gut Fluid Conditions Is Biphasic and Reversible. *Environ. Sci. Technol.* **2019**, *53*, 1874–1883. https://doi.org/10.1021/acs.est.8b05143.

(52) Gouin, T.; Roche, N.; Lohmann, R.; Hodges, G. A Thermodynamic Approach for Assessing the Environmental Exposure of Chemicals Absorbed to Microplastic. *Environ. Sci. Technol.* **2011**, *45* (4), 1466–1472.

(53) Koelmans, A. A.; Bakir, A.; Burton, G. A.; Janssen, C. R. Microplastic as a Vector for Chemicals in the Aquatic Environment: Critical Review and Model-Supported Reinterpretation of Empirical Studies. *Environ. Sci. Technol.* **2016**, *50* (7), 3315–3326. https://doi.org/10.1021/acs.est.5b06069.

(54) Groh, K. J.; Backhaus, T.; Carney-Almroth, B.; Geueke, B.; Inostroza, P. A.; Lennquist,

A.; Leslie, H. A.; Maffini, M.; Slunge, D.; Trasande, L.; Warhurst, A. M.; Muncke, J. Overview of Known Plastic Packaging-Associated Chemicals and Their Hazards. *Science of the Total Environment*. 2019. https://doi.org/10.1016/j.scitotenv.2018.10.015.

(55) Li, S. Q.; Ni, H. G.; Zeng, H. PAHs in Polystyrene Food Contact Materials: An Unintended Consequence. *Sci. Total Environ.* **2017**. https://doi.org/10.1016/j.scitotenv.2017.07.262.

(56) Chen, G.; Feng, Q.; Wang, J. Mini-Review of Microplastics in the Atmosphere and Their Risks to Humans. *Science of the Total Environment*. 2020. https://doi.org/10.1016/j.scitotenv.2019.135504.

(57) Ogawara, K. ichi; Yoshida, M.; Kubo, J. ichi; Nishikawa, M.; Takakura, Y.; Hashida, M.; Higaki, K.; Kimura, T. Mechanisms of Hepatic Disposition of Polystyrene Microspheres in Rats: Effects of Serum Depend on the Sizes of Microspheres. *J. Control. Release* **1999**, *61* (3), 241–250. https://doi.org/10.1016/S0168-3659(99)00121-2.

(58) Li, M.; Panagi, Z.; Avgoustakis, K.; Reineke, J. Physiologically Based Pharmacokinetic Modeling of PLGA Nanoparticles with Varied MPEG Content. *Int. J. Nanomedicine* **2012**, *7*, 1345–1356. https://doi.org/10.2147/IJN.S23758.

(59) Bachler, G.; von Goetz, N.; Hungerbühler, K. A Physiologically Based Pharmacokinetic Model for Ionic Silver and Silver Nanoparticles. *Int. J. Nanomedicine* **2013**, *8* (1), 3365–3382. https://doi.org/10.2147/IJN.S46624.